arXiv:1110.1683v1 [cond-mat.stat-mech] 8 Oct 2011

Crystalline and quasicrystalline local order in a model polymer melt

S. Bernini and F. Puosi
Dipartimento di Fisica “Enrico Fermi”, Università di Pisa, Largo B.Pontecorvo 3, I-56127 Pisa, Italy

D. Leporini*
Dipartimento di Fisica “Enrico Fermi”, Università di Pisa, Largo B.Pontecorvo 3, I-56127 Pisa, Italy and
IPCF-CNR, UOS Pisa, Italy
(Dated: October 11, 2011)

We investigate by Molecular-Dynamics methods the local order in a melt of a fully-flexible polymer chains. Evidence is given of clusters with well-defined crystalline and quasi-crystalline order.

PACS numbers:
Keywords:

I. INTRODUCTION

There is growing interest in the possible presence of localized ordered structures in liquids and polymeric systems [1, 2]. Here we present the preliminary report of a thorough numerical study of these issues in polymer melts. By careful analysis of both the positional and the angular features of the inherent structures [3], evidence is given of clusters with well-defined crystalline and quasi-crystalline order, i.e. face-centered cubic (fcc) , hexagonally close-packed (hcp) and icosahedral (icos) order.

The paper is organized as follows. In Sec. II the polymer model and the Molecular-Dynamics (MD) algorithms are presented. The results are discussed in Sec.III. Finally, the main conclusions are summarized in Sec.IV.

II. METHODS

A. Details of simulations

A coarse-grained model of a melt of linear fully-flexible unentangled polymer chains with fixed bond lenght and M monomers each is used. The system has $N = 500$ monomers in all cases but $M = 3$, where $N = 501$. Nonbonded monomers at a distance r belonging to the same or different chains interact via a truncated LJ potential:

$$U_{LJ}(r) = \epsilon \left[\left(\frac{\sigma^*}{r} \right)^{12} - 2 \left(\frac{\sigma^*}{r} \right)^{6} \right] + U_{cut} \qquad (1)$$

where $\sigma^* = 2^{1/6}\sigma$ is the position of the potential minimum with depth ϵ, and the value of the constant U_{cut} is chosen to ensure $U_{q,p}(r) = 0$ at $r \geq r_c = 2.5\,\sigma$. Bonded monomers are costrained to a distance $b = 0.97\,\sigma$ by using the RATTLE algorithm [4]. All quantities are in reduced units: lenght in units of σ, temperature in units of ϵ/k_B and time in units of $\sigma\sqrt{\mu/\epsilon}$ where μ is the monomer mass. We set $\mu = k_B = 1$. States with different values of the temperature T, the density ρ and the chain lenght M; each state is labelled by the multiplet $\{M, \rho, T\}$. NPT and NTV ensembles have been used for equilibration runs, while NVE ensemble has been used for production runs for a given state point. NPT and NTV ensembles are studied by the extended system method introduced by Andersen [5] and Nosé [6]. The numerical integration of the augmented Hamiltonian is performed through the multiple time steps algorithm, reversible Reference System Propagator Algotithm (r-RESPA), developed by Tuckerman *et al* [7]. In particular, the NPT and NTV operators is factorized using the Trotter theorem [8] separating the short range and long range contributions of the potential, according to the Weeks-Chandler-Andersen (WCA) decomposition [9].

B. Inherent configurations

At non-zero temperature monomers vibrate around their equilibrium positions; such fast movements make it difficult to characterize the arrangement of monomers. In order to remove vibrations one usually resorts to the so-called inherent structures (IS) by mapping the configurations of the simulated trajectory into the corresponding local minimum of the potential energy [3]. The conjugate-gradient method is used to minimize the configurational energy as a function of the $3N$ particles coordinates [10]. Henceforth, a physical quantity X will be denoted as X^{IS} if evaluated in terms of IS configurations.

III. RESULTS AND DISCUSSION

A. Radial distribution function

First, the radial distribution function $g(r)$ of the system is considered. In a polymer system the function $g(r)$ can be naturally separated into the intrachain part $g_{ic}(r)$ and the interchain part $g_{ex}(r)$.

In Figure 1 the intrachain part of the radial distribution function $g_{ic}^{IS}(r)$ is shown for trimers ($M = 3$) at different temperatures. The less-resolved instantaneous $g(r)$ is

---

*Electronic address: dino.leporini@df.unipi.it

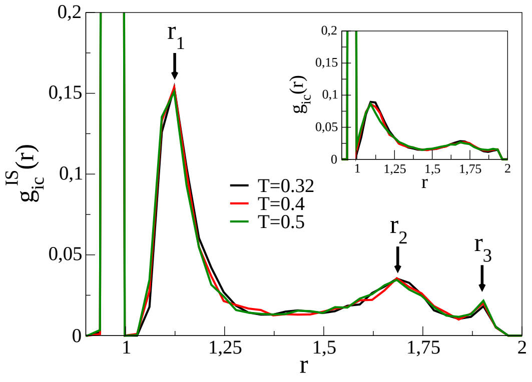

FIG. 1: Intrachain part of the inherent radial distribution function $g_{ic}^{IS}(r)$ for trimers ($M = 3$) with density $\rho = 0.984$ at the indicated temperatures. Inset: corresponding instantaneous intrachain radial distribution function $g_{ic}(r)$.

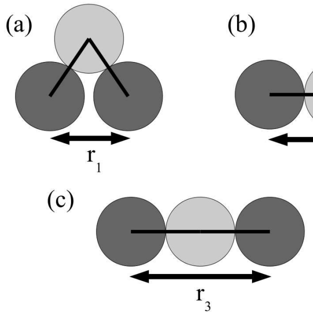

FIG. 2: Monomer arrangements corresponding to the three peaks of the intrachain part of the radial distribution function in Fig.1. Distance r and bond-bond angle θ refer to the dark monomers. a) folded conformation ($r_1 \approx 1.12$, $\theta_1 \approx 70°$); b) partially folded conformation ($r_2 \approx 1.69$, $\theta_2 \approx 120°$); c) linear conformation ($r_3 \approx 1.94$, $\theta_3 \approx 180°$).

also plotted. Bonded monomers give a δ-like contribution at $r = b = 0.97$. For larger distances, three peaks at r_1, r_2 and r_3 are apparent. Figure 2 shows the arrangements of the three bonded monomers resulting in the distances r_1, r_2 and r_3. The first and highest peak of $g_{ic}^{IS}(r)$ at $r_1 \approx 1.12$ corresponds to folded trimers in which the two chain ends are at a distance $r_1 = \sqrt[6]{2} \approx 1.12$, the position of the minimum of the Lennard-Jones potential. The central peak at $r_2 \approx 1.69$ corresponds to the partially-folded conformation with two consecutive bonds forming an angle $\theta \approx 120°$. The third peak at $r_3 \approx 2b \approx 1.94$ signals trimers with linear conformations.

The conformations plotted in Fig.2 are observed also in longer chain (not shown).

In the panel (a) of Figure 3 the interchain part of the radial distribution function $g_{ex}^{IS}(r)$ is shown for trimers at different temperatures. The most interesting feature is the split of the second-neighbors peak in three sub-peaks (enlargement in panel (b)), a feature which is apparent only in IS configurations and is missing in the instantaneous configurations

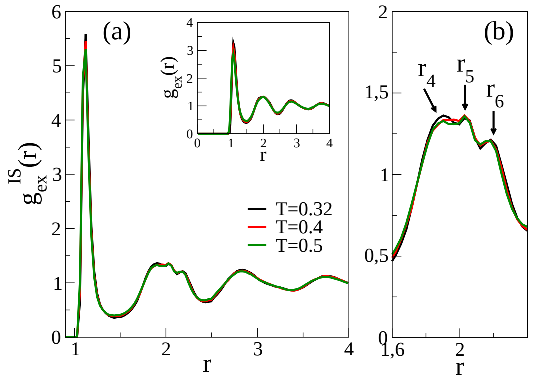

FIG. 3: Panel (a): Interchain part of the inherent radial distribution function $g_{ex}^{IS}(r)$ for trimers $M = 3$ with density $\rho = 0.984$ at the indicated temperatures. Inset: corresponding instantaneous interchain part of the radial distribution function $g_{ex}(r)$. Panel (b): Enlargement of the second-neighbors peak of $g_{ex}^{IS}(r)$. Note that the peak is resolved only by considering IS configurations (compare with the inset of panel a)).

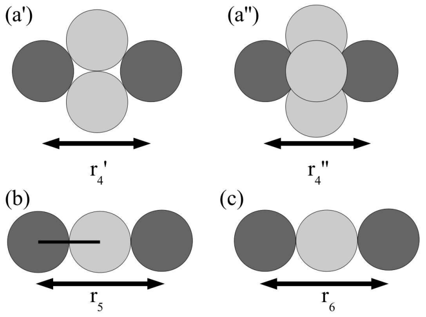

FIG. 4: Monomer arrangements corresponding to the three subpeaks of the second-neighbors peak of $g_{ex}^{IS}(r)$. The distance is measured between the dark monomers. Bonds (black straight lines) are not shown if not relevant. Adjacent triangle (a') and face-sharing tetrahedra (a") ($r_4' \approx r_4'' \approx 1.9$); b): three linear monomers, two bonded ($r_5 \approx 2.05$); c): three linear nonbonded monomers ($r_6 \approx 2.2$).

(Fig,3a, inset). The arrangements of the monomers corresponding to the three sub-peaks of the second-neighbors peak of $g_{ex}^{IS}(r)$ are shown in Figure 4. The two side sub-peaks at $r_4 \approx 1.9$ and $r_6 \approx 2.2$, already observed in atomic systems [11], signal two monomers separated by other overlapping monomers and three monomers in a linear conformation, respectively. In both cases the arrangements involve only nonbonded monomers. The central sub-peak at $r_5 \approx 2.05$ is peculiar of the polymer system and marks a linear arrangement of three monomers, two of them being bonded. For longer chains, the two side peaks vanish while the central peak increases slightly (not shown).

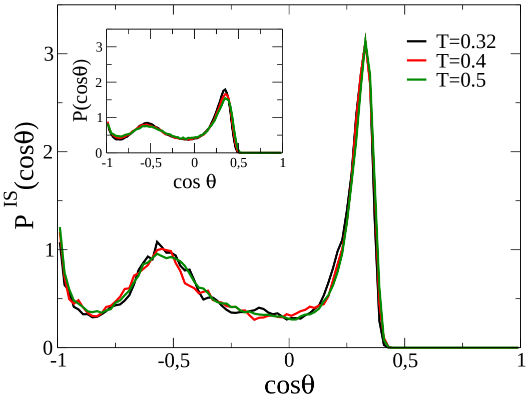

FIG. 5: Inherent distribution of the bond-bond angle $P^{IS}(\cos\theta)$ for trimers with density $\rho = 0.984$ at the indicated temperatures. Inset: corresponding instantaneous distribution $P(\cos\theta)$.

B. Bond-bond angle distribution

Further information on the local structure is gained by the distribution of the angle between adjacent bonds in a chain, $P(\cos\theta)$. In Figure 5 the distribution $P^{IS}(\cos\theta)$ for trimers is shown. Again, IS configurations yield better resolution with respect to the instantaneous ones (Fig.5, inset). The distribution vanishes above $\cos\theta \approx 0.5$ since monomers cannot overlap. It is easily seen that the peaks of $P^{IS}(\cos\theta)$ at $\theta_1 \approx 70°$, $\theta_2 \approx 120°$ and $\theta_3 \approx 180°$ originate from the dominant conformations evidenced by the intrachain part of the radial distribution function (Figure 2).

C. Orientational order

The radial pair distribution function $g(r)$ provides only orientationally-averaged information on the arrangements of the monomers surrounding a given one. To gain insight into their orientational distribution, we resort to the rotational invariant measures Q_l [12].

We consider the spherical polar angles $\theta(\mathbf{r})$ and $\phi(\mathbf{r})$ of the vector $\mathbf{r}$ joining a central monomer with one of the n_b neighbors within a cutoff distance $r^* \approx 1.25\sigma^*$. A spherical harmonic $Y_{lm}[\theta(\mathbf{r}), \phi(\mathbf{r})]$ is associated to these angles. The quantity $\bar{Q}_{lm}$ is defined as:

$$\bar{Q}_{lm} = \frac{1}{n_b} \sum_{i=1}^{n_b} Y_{lm}[\theta(\mathbf{r}_i), \phi(\mathbf{r}_i)] \qquad (2)$$

The orientational order parameter Q_l is then defined as:

$$Q_l = \left(\frac{4\pi}{(2l+1)} \sum_{m=-l}^{l} |\bar{Q}_{lm}|^2 \right)^{1/2} \qquad (3)$$

In the absence of orientational order $Q_l = 0, \forall l \neq 0$. The Q_l values for different kinds of orientational order are easily computed. In Figure 6 several order parameters are shown for three clusters of 13 particles with pure icosahedral (icos), face centered cubic (fcc) and hexagonally close-packed (hcp) order. Non-zero values appear for $l \geqslant 4$ in the fcc and hcp clusters while in the icosahedral cluster non-zero values occur only for $l = 6$ and $l = 10$.

The orientational order parameters Q_l^{IS} for $l = 2, 4, 6, 8, 10$ are shown in Figure 7 for IS configurations of trimers $M = 3$ (upper panel) and decamers $M = 10$ (lower

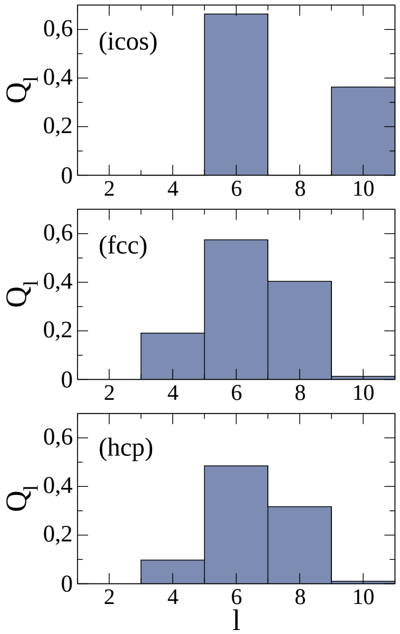

FIG. 6: Orientational order parameters Q_l for 13-particles clusters with pure icosahedral (icos), face-centered cubic (fcc) and hexagonally close-packed (hcp) order.

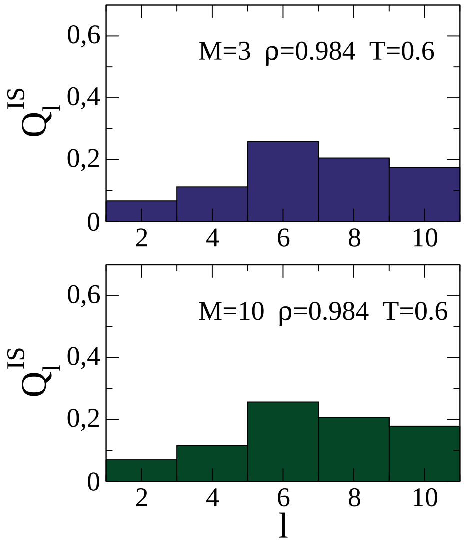

FIG. 7: Orientational order parameters Q_l^{IS} for IS configurations of trimers ($M = 3$) and decamers ($M = 10$) at density $\rho = 0.984$ and temperature $T = 0.6$.

panel). The presence of icosahedral orientational order is signaled by $Q_{10} \neq 0$. However, the non-zero values of Q_l for $l = 4, 8$, which vanish under icosahedral symmetry, indicate the presence of partial fcc and hcp orientational order too.

It is easily seen that the positional and the angular features evidenced by the analysis of the radial distribution function and the bond-bond angle distribution in Sections III A and III B are further evidence of the different kinds of orientational order shown by the orientational order parameters. Finally, one notes that the order parameters Q_l are coincident for trimers and decamers, thus suggesting that the increasing connectivity does not affect the local order in a marked way.

IV. CONCLUSIONS

By analysing the positional and the angular features of the IS radial distribution function and bond-bond angle distribution as well as the local orientational order parameters, we evidenced the presence of clusters with crystalline (hcp and fcc) and quasi-crystalline order in a melt of fully-flexible polymer chains.

---

[1] N. C. Karayiannis, K. Foteinopoulou, and M. Laso, J. Chem. Phys. **130**, 164908 (2009).

[2] M. Asai, M. Shibayama, and Y. Koike, Macromolecules **44**, 6615 (2011).

[3] F. Stillinger, Science **267**, 1935 (1995).

[4] M. P. Allen and D. J. Tildesley, *Computer simulations of liquids* (Oxford university press, Clarendon, 1987).

[5] H. C. Andersen, J. Chem. Phys. **72**, 2384 (1980).

[6] S. Nosé, J. Chem. Phys. **81**, 511 (1984).

[7] M. E. Tuckerman, B. J. Berne, and G. J. Martyna, J. Chem. Phys. **97**, 1990 (1992).

[8] H. F. Trotter, Proc. Am. Math. Soc. **10**, 545 (1959).

[9] M. E. Tuckerman, B. J. Berne, and G. J. Martyna, J. Chem. Phys. **94**, 6811 (1991).

[10] W. Press, B. Flannery, S. Teukolsky, and W. Vetterling, *Numerical Recipes in C: The Art of Scientific Computing* (Cambridge University Press, 1987).

[11] A. Clarke and H. Jónsson, Phys. Rev. E **47**, 3975 (1993).

[12] P. Steinhardt, D. Nelson, and M. Ronchetti, Phys. Rev. B **28**, 784 (1983).